9

Slope Error and Surface Roughness

F. Siewert

Abstract. This chapter describes the diffraction theory relationships between figure errors of grazing incidence mirrors and their imaging performance at synchrotron radiation beam lines. A practical illustrative example is the topographic errors of a synchrotron mirror as a function of spatial frequency. The basic idea of figure error inspection by direct slope measurement is described.

Mirrors of high shape accuracy used in grazing incidence are essential to focus or collimate the light in synchrotron radiation (SR) beamlines. Thus, many of the synchrotron laboratories have been established the expertise and equipment to measure the critical characteristics of high performance optical elements. Better knowledge describing the shape of an optical element allows better modeling, optimization, and in the final analysis, performance of optical systems. The quality of reflective optical elements can be described by their deviation from ideal shape at different spatial frequencies. Usually one distinguishes between the figure error, the low spatial error part ranging from aperture length to 1 mm frequencies, and the mid- and high spatial error part from 1 mm to 1 µm and from 1 µm to some 10 nm spatial frequencies, respectively [1, 2]. While the figure error will affect the imaging properties of the system the higher spatial frequency errors will cause light to be deflected or scattered away from the spectral image. The quantitative description of the surface errors of a reflecting optical element can be statistically interpreted in terms of power spectral density function, PSD, and summarized as the slope error and the surface roughness. Based on Kirchhoff's theory of diffraction, Church and Takacs [2, 3] have developed a model to describe this (see also [4, 5]). The natural "system coherence length," W, is given by

$$W = \sqrt{2}\frac{\lambda}{\Theta \cos\theta_{\mathrm{i}}} \tag{9.1}$$

with Θ as the angular radius of the system image (customer given), θ_{i} is the angle of incidence relative to the mirror plane, and λ is the operating

wavelength. W is the surface spatial wavelength that diffracts to the $1/e$ intensity point in a Gaussian system image [2, 3]. In the case of diffraction limited optical elements W is approximately the length of the illuminated area of the mirror of the length L. In the case of system limited optical components assumed here it is much less than L [2]. In the case of synchrotron optics W is a wavelength between the spatial wavelengths ranging from λ to L. We assume that the influence of the mirror errors on the image quality can be described by the on-axis Strehl factor for the grazing incidence case, (1.3) [2]. The on-axis Strehl factor

$$\frac{I(0)}{I_0(0)} \tag{9.2}$$

is given as the ratio of the on-axis intensity in the presence of real surface errors to its value for zero errors. For the grazing incidence case can be written [2]:

$$\frac{I(0)}{I_0(0)} \approx 1 - \frac{8}{\Theta^2}\delta^2 - \left(\frac{4\pi}{\lambda}\cos\theta_\mathrm{i}\right)^2 \sigma^2, \tag{9.3}$$

where δ and σ are the bandwidth limited values of the rms values of the slope error (δ) and the roughness (σ) given by [2]

$$\delta^2 = (2\pi)^2 \int_{1/L}^{1/W} \mathrm{d}f_x S_1(f_x) f_x^2 \tag{9.4}$$

and

$$\sigma^2 = \int_{1/W}^{1/\lambda} \mathrm{d}f_x S_1(f_x). \tag{9.5}$$

$S_1\,(f_x)$ is the profile spectrum of the surface under test (SUT).

The surface roughness can be measured using an interferometric microscope or atomic force microscope (AFM). To inspect the slope error, a different measuring technique is used: interferometry or various types of surface profilers. The use of an interferometer, to inspect optical components, requires a reference of complementary shape and excellent quality. Due to the fact that many of the necessary optical components are of aspherical shape and are designed individually for each SR-beamline, such reference objects would cause an extraordinary expense for the metrology. In addition, the quality of the references used limits the accuracy of the result of the metrology. Because of the flat (grazing) angles used in SR-beamlines, synchrotron mirrors may have a length of up to 1 m and more and have a large ratio of length to width. Thus, basic conditions have lead to the idea of inspecting the shape of optical elements in the long dimension by slope measurement. A few slope measuring instruments have been developed during the last two decades, foremost among them, the long trace profiler (LTP) [6, 7], and recently the nanometer optical component measuring machine (NOM) [8, 9] and the extended shear angle difference method (ESAD) [10, 11]. These methods are based on the principle of direct measurement of slope deviation and curvature and, in contrast to

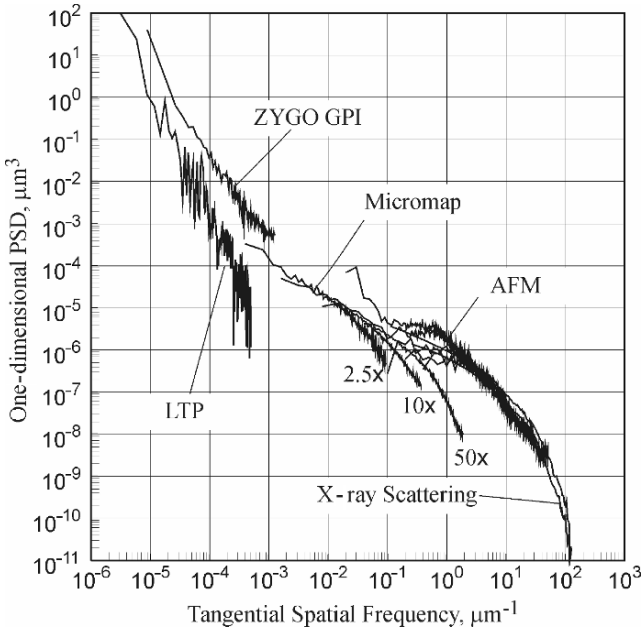

Fig. 9.1. Different measuring instruments cover different ranges of spatial frequency. Tangential 1D PSD spectra obtained with the 6-in ZYGO-GPI^{TM} interferometer, the LTP-II, the Micromap-570TM, the AFM and the CXRO reflectometry and scattering experimental facility at the advanced light source (ALS). The figure is a compilation of data published in [5, 12] (courtesy of Valeriy V. Yashchuk, LBNL/ALS)

other methods, yield results without the need for a reference. The measurement result is directly traced back to SI base units angle and length (SI – is the International System of Units). The measurement is a noncontact scan by using a laser source to create a measurement beam. Depending on the angular acceptance of the instrument, it is possible to measure the geometry of any reflective surface.

Figure 9.1 shows the range of spatial frequencies to be inspected by using different metrological instruments [5]. In the case shown, a stainless steel mirror was investigated using different measuring techniques over a spatial frequency range from $\sim 10^{-6}$–$10^{-2}\,\mu$m [5, 12].

9.1 The Principle of Slope Measurements

To measure the shape of an optical element a test beam from a laser source is reflected from the SUT. The relative position after reflection from the SUT is determined by the local shape and is detected on a sensor. The reflection of a test beam from a mirror along the axis of the instrument will depend on

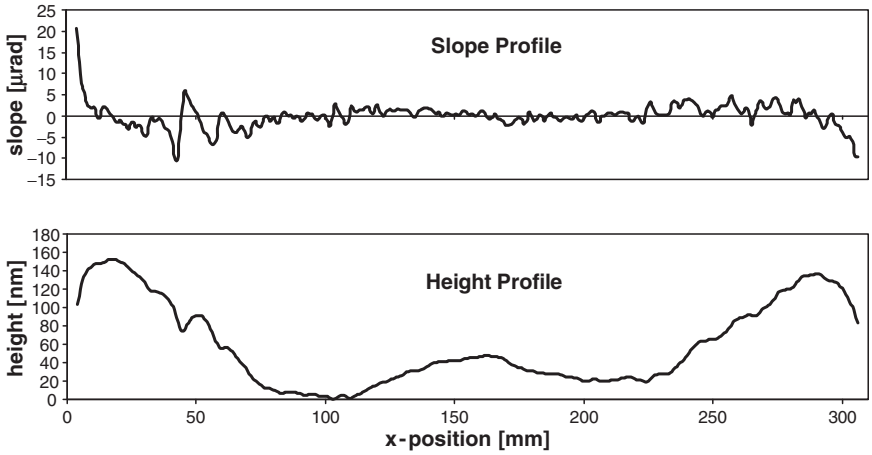

Fig. 9.2. Result of a direct slope measurement (NOM-scan): slope profile of a plane mirror (*top*) and the corresponding profile of height (*below*), obtained by integration of the slope data

the angle θ, of the mirror's normal with respect to the propagation direction of the laser beam [13, 14]. The slope δ is

$$\delta(x) = \tan\theta = \mathrm{d}y/\mathrm{d}x. \tag{9.6}$$

Of interest is the relative slope along the line of inspection. What is detected in the sensor is the change in angle of reflection from one position, x, on the SUT to the next position, $x + \Delta x$. From these data the height profile can be obtained by an integration of the slope function $\delta(x)$ over the abscissa x, see also Fig. 9.2. The height function is given by

$$h(x) = \int_{x=\mathrm{scanstart}}^{x=\mathrm{scanstop}} \delta(x)\mathrm{d}x \tag{9.7}$$

The commonly used criteria for the characterization of the shape quality is the figure slope error or residual slope error, obtained by subtracting the profile for the theoretically perfect geometry from the raw slope data.

Acknowledgments

The author gratefully acknowledges Daniele Cocco (Elettra) and Valeriy V. Yashchuk (ALS) for helpful discussions.

References

1. J.S. Taylor, G.E. Sommargren, D.W. Sweeney, R.M. Hudyama, UCRL-JC-128290 Rev. **1** (1998)
2. E.L. Church, P.Z. Takacs, Opt. Eng. **34**(2), 353 (1995)

3. E.L. Church, P.Z. Takacs, Appl. Optics **32**(19), 3344 (1993)
4. V.V. Yashchuk, M.R. Howells, W.R. McKinney, P.Z. Takacs, in *Proceedings of The 3rd International Workshop on Metrology for X-Ray Optics*, Daegu, 2006
5. V.V. Yashchuk, S.C. Irick, E.M. Gullikson, M.R. Howells, A.A. MacDowell, W.R. McKinney, F. Salmassi, T. Warwick, in *Advances in Metrology for X-Ray and EUV Optics*, ed. by L. Assoufid, P.Z. Takacs, J.S. Taylor, Proceedings of SPIE, vol. 5921, 2005, p. 18
6. P. Takacs, S. Qian, J. Colbert, SPIE **749**, 59 (1987)
7. P.Z. Takacs, S.-N. Qian, United States Patent 4,884,697, 1989
8. F. Siewert, T. Noll, T. Schlegel, T. Zeschke, H. Lammert, in *AIP Conference Proceedings*, vol. 705, Mellvile, New York, 2004, p. 847
9. H. Lammert, T. Noll, T. Schlegel, F. Siewert, T. Zeschke, in *Patentschrift DE10303659 B4 2005.07.28*
10. I. Weingärtner, M. Schulz, C. Elster, in *Proceedings of SPIE*, vol. 3782, 1999, p. 306
11. C. Elster, I. Weingärtner, Appl. Opt. **38**, 5024 (1999)
12. V.V. Yashchuk, S.C. Irick, E.M. Gullikson, M.R. Howells, A.A. MacDowell, W.R. McKinney, F. Salmassi, T. Warwick, *Advances in Metrology for X-Ray and EUV Optics*, ed. by L. Assoufid, P.Z. Takacs, J.S. Taylor, Proceedings of SPIE, vol. 5921, 2005, p. 18
13. S.C. Irick, Rev. Sci. Instrum. **63**(1), (1992)
14. R. Signorato, M. Sanchez del Rio, in *Proceedings of SPIE*, vol. 3152, 1997, p. 136